



# Thermal stability assessment of nitrocellulose by using multiple calorimetric techniques and advanced thermokinetics

Yan Tang<sup>1</sup> · Zhi-Ping Li<sup>1</sup> · Hai-Lin Zhou<sup>2</sup> · Chun-Feng Miao<sup>3</sup> · Jun-Cheng Jiang<sup>1</sup> · An-Chi Huang<sup>1</sup>

Received: 29 June 2022 / Accepted: 21 October 2022 / Published online: 15 November 2022  
© Akadémiai Kiadó, Budapest, Hungary 2022

## Abstract

Nitrocellulose is a typical nitro-energetic material that has been widely used in civil and military fields; however, its high flammability and explosibility have made it the main hazard factor in many industrial accidents. Understanding the thermal characteristics of this material is the basis for effective hazard control. Therefore, we investigated the thermal stability parameters of nitrocellulose by using multiple calorimetric techniques (thermogravimetry, differential scanning calorimetry, and adiabatic accelerating calorimetry). The Friedman, Flynn–Wall–Ozawa, Kissinger–Akahira–Sunose, Starink, and Vyazovkin thermokinetic methods were used to analyze the activation energy of nitrocellulose under different oxygen contents (0%, 5%, 10%, 15%, and 21%). In addition, the mechanisms of thermal decomposition, adiabatic temperature rise, time to conversion limit, and self-accelerating decomposition temperature were determined. The results reveal that the thermal decomposition of nitrocellulose in a nitrogen atmosphere was a one-step autocatalytic reaction. The activation energy under different oxygen contents showed an “increase–stabilize–decrease” trend during thermal decomposition. The findings of this study can serve as a reference for the suitable production, storage, transportation, and usage of nitrocellulose.

**Keywords** Thermal decomposition · Reaction kinetics · Adiabatic temperature rise · Time to conversion limit · Self-accelerating decomposition temperature

## List of symbols

$A$	Frequency factor ( $1\text{ s}^{-1}$ )	$\Delta T_{\text{ad}}$	Adiabatic temperature rise ( $^{\circ}\text{C}$ )
$E_a$	Apparent activation energy ( $\text{kJ mol}^{-1}$ )	$f(\alpha)$	Differential form of reaction mechanism function
$T$	Absolute temperature (K)	$G(\alpha)$	Integral form of reaction mechanism function
$M$	Sample mass (mg)	$R$	Universal gas constant [ $8.314\text{ J (mol K)}^{-1}$ ]
$m_0$	Initial mass of sample (mg)	$R^2$	Coefficient of determination
$m_e$	Final mass of sample (mg)	$C_K$	Constant for Kissinger method
$t$	Time (s)	$C_O$	Constant for Ozawa method
$k$	Reaction rate constant	$C_B$	Constant for Boswell method
$T_0$	Onset temperature ( $^{\circ}\text{C}$ )	$C_s$	Constant for Starink method
$T_p$	Peak temperature ( $^{\circ}\text{C}$ )	TCL	Time to conversion limit (day)
$\Delta H$	Heat of reaction ( $\text{J g}^{-1}$ )	TMR	Time to the maximum reaction rate (day)
		SADT	Self-accelerating decomposition temperature ( $^{\circ}\text{C}$ )
		$\phi$	Factor of thermal inertia
		$\alpha$	Conversion rate
		$\beta$	Heating rate ( $^{\circ}\text{C min}^{-1}$ )

✉ Jun-Cheng Jiang  
jiangjc@cczu.edu.cn

✉ An-Chi Huang  
huangac@cczu.edu.cn

<sup>1</sup> School of Environmental and Safety Engineering, Changzhou University, Changzhou 213164, Jiangsu, China

<sup>2</sup> School of Material Science and Engineering, Changzhou University, Changzhou 213164, Jiangsu, China

<sup>3</sup> College of Safety Science and Engineering, Nanjing Tech University, Nanjing 210009, Jiangsu, China

## Introduction

Nitrocellulose is a typical nitro-energetic material that can be prepared through the esterification of cellulose and nitric acid [1, 2]. This material is currently widely used in civil and military fields to produce paints, films, plastics, explosives,

and rocket propellants [3–6]. However, nitrocellulose has been the main hazard factor in many industrial accidents because of its high flammability and explosibility. The thermal runaway of nitrocellulose has caused many disasters, such as the ones in Shinagawa Ward (July 14, 1964), Zhongshan (August 16, 2006), Xingtai (January 24, 2014), and Tianjin (August 12, 2015) [3, 7–9]. The worst tragedy in recent years was the fire and explosion at Tianjin port, in which 165 people died, eight people were lost, and 798 people were injured. In addition, the direct economic loss caused by this accident was RMB6.866 billion. The hazardous properties of nitrocellulose dramatically limit its applications, and the associated thermal safety issues have been studied extensively by scholars worldwide [10–15].

Many researchers have investigated the thermal hazard of nitrocellulose in terms of its decomposition, combustion, and explosion characteristics. Kinetic analysis has been conducted often in such studies, and the parameters of the Arrhenius equation have been obtained, which are crucial for evaluating the safety level of nitrocellulose in its manufacturing, storage, and transportation [5, 10, 16–18]. Pourmortazavi et al. investigated the thermochemical behavior of nitrocellulose samples with different nitrate contents and obtained the activation energy, frequency factor, and critical explosion temperature of nitrocellulose [1]. Lin et al. computed the activation energy of nitrocellulose during its thermal decomposition by conducting thermogravimetric analysis (TGA) and differential scanning calorimetry (DSC) experiments. In addition, they compared the data fitting results obtained using these two methods [13]. Wang et al. found that the thermal decomposition of nitrocellulose satisfied the first-order equation, and on the basis of this information, they computed the critical explosion temperature and activation energy [19]. He et al. investigated the effects of humectants on the activation energy of nitrocellulose decomposition in a nitrogen atmosphere. The results indicated that nitrocellulose with isopropanol had higher activation energy and stability than that with ethanol or without a humectant [20]. Luo et al. studied the decomposition characteristics of nitrocellulose in air and computed its activation energy under different conversion rates [21]. Mi analyzed the thermal stabilities of fiber and chip nitrocellulose and found that the activation energy ratio of these two forms was 1.6 [22]. Wei et al. investigated the effect of aging time on the kinetic parameters of nitrocellulose by using a TG–DSC analyzer. The results indicated that minimum parameters values were achieved under an aging time of 24 days and an aging temperature of 90 °C [23]. Gao et al. studied the thermal kinetics and reaction mechanism of nitrocellulose pyrolysis in a nitrogen atmosphere. The relationship between activation energy and conversion was obtained by multi-kinetics and the reaction model was reconstructed [2]. Yang et al. investigated effect of metal chloride on the thermal decomposition

of nitrocellulose and found that divalent metal chlorides can increase the activation energy and pre-exponential factor of nitrocellulose, whereas trivalent metal chlorides have the opposite effects [9].

In the literature, extensive investigations and useful conclusions pertaining to the thermal stability and runaway characteristics of nitrocellulose have been reported. However, in these investigations, kinetic parameters were obtained mainly in nitrogen or air atmospheres, the oxygen contents of which are 0% and 21%, respectively. In real conditions, nitrocellulose is often stored and transported in confined spaces. If fires occur in such places, the combustion of a massive quantity of nitrocellulose results in the rapid consumption of oxygen, which cannot be easily replaced by air from the external environment. For example, the Tianjin accident occurred because of the combustion of nitrocellulose stored in a container, which represents an oxygen-lean environment ( $0% < O_2\% < 21%$ ). Oxygen content has a crucial influence on kinetic parameters [24, 25]; however, few studies have investigated the thermal characteristics of nitrocellulose under oxygen-lean conditions. Therefore, in the present study, we used a thermogravimetric analyzer in conjunction with multiple thermokinetic methods, namely the Friedman, Flynn–Wall–Ozawa (FWO), Kissinger–Akahira–Sunose (KAS), Starink, and Vyazovkin methods, to obtain the activation energy ( $E_a$ ) values of nitrocellulose under various oxygen contents. A differential scanning calorimeter and an adiabatic accelerating calorimeter (ARC) were used to analyze the thermal characteristics of nitrocellulose. Critical thermal stability parameters such as adiabatic temperature rise, time to conversion limit, and self-accelerating decomposition temperature were determined to evaluate the thermal hazards of nitrocellulose. The findings of this study can further deepen the understanding regarding nitrocellulose and serve as a reference for its suitable production, storage, transportation, and usage.

## Experimental

### Sample preparation

In the experiments conducted in this study, we used samples of floccule-type nitrocellulose with a nitrogen content of 11.5–12.2%. Ethyl alcohol with a content of 30% was used as the humectant to prevent possible spontaneous combustion. The samples were sealed and stored in an anti-explosion refrigerator at temperatures of 2–6 °C.

### Thermogravimetric analysis

TGA, which is a typical thermal analysis technology, was used in this study to obtain the relationship between material

mass and temperature. In our experiments, we used TGA 2 (Mettler Toledo Co., Zurich, Switzerland) to determine the thermodynamic behavior of the samples. The original mass of the samples was  $7.44 \pm 0.07$  mg. The temperature of the samples was increased from 30.0 to 300.0 °C under heating rates of 2.0, 4.0, 6.0, 8.0, and 10.0 °C min<sup>-1</sup>. An oxygen-lean environment was created precisely by using two mass-flow control instruments (Alicat, America). Oxygen contents of 0%, 5%, 10%, 15%, and 21% were achieved by controlling the mass flows of oxygen and nitrogen separately. The oxygen and nitrogen flows were then combined and input into the thermogravimetric analyzer at a total gas flow rate of 50 mL min<sup>-1</sup>.

### Differential scanning calorimetry

The sample in TG experiment was tested in an open environment while the DSC experiment was performed in a sealed crucible; hence, DSC experiments were carried out in this paper as a reference in analyzing the thermal stability of samples. In the DSC experiments, the relationship between heat flux and temperature was obtained by measuring the flux difference between the samples and reference materials during a temperature-programmed process. A DSC 3 (Mettler Toledo Co., Greifensee, Switzerland) instrument was used to analyze the thermal decomposition reaction of nitrocellulose. The samples were heated from 30.0 to 300.0 °C at rates of 2.0, 4.0, 6.0, 8.0, and 10.0 °C min<sup>-1</sup> in a nitrogen atmosphere. The mass of the samples was  $2.05 \pm 0.03$  mg, and the nitrogen gas flow rate was 50 mL min<sup>-1</sup>.

### Adiabatic accelerating calorimetry

Adiabatic accelerating calorimeters possess a "Heat–Wait–Search" mode for measuring the temperature, enthalpy, and pressure of a chemical reaction in an adiabatic environment. Therefore, we conducted adiabatic accelerating calorimetry experiments to supplement the TGA and DSC tests. An ARC 244 (Netzsch, Selb, Germany) instrument was used to measure the temperature and pressure of the samples. The sample mass was 102 mg, and the samples were tested in a Hastelloy sample container. In the ARC experiments, the temperature was increased from 120 to 300 °C under a heating rate of 10.0 °C min<sup>-1</sup>.

### Thermokinetic models

According to the theory of thermal analysis, kinetic analysis methods can be categorized as isothermal and non-isothermal methods. Moreover, non-isothermal methods can be subdivided into single-heating-rate and multiple-heating-rate methods [24, 26]. These non-isothermal methods with multiple heating rates, which are also called iso-conversional

or model-free methods, have been paid more attention as they can be used to obtain reliable activation energy values without reaction mechanism functions [24, 27, 28]. Therefore, we adopted typical model-free methods (the Friedman, FWO, KAS, Vyazovkin, and Starink methods) to calculate the activation energy of nitrocellulose under different oxygen contents. The details of these methods are provided in the following text.

#### Friedman method

The Friedman kinetic model is based on a single-step kinetic mechanism, and this model can be derived from the following equations in a progressive manner [29–31]:

$$\alpha = \frac{m_0 - m}{m_0 - m_e} \quad (1)$$

$$\frac{d\alpha}{dt} = kf(\alpha) \quad (2)$$

$$k = A \exp\left(-\frac{E_a}{RT}\right) \quad (3)$$

$$\ln\left(\frac{d\alpha}{dt}\right) = \ln[Af(\alpha)] - \frac{E_a}{RT} \quad (4)$$

where  $\alpha$  is the conversion rate at a certain time;  $m$  is the sample mass;  $m_0$  and  $m_e$  represent the mass at the start and end points;  $t$  denotes the time;  $k$  denotes the reaction rate;  $f(\alpha)$  represents the reaction model;  $A$  and  $E_a$  are Arrhenius parameters that represent the pre-exponential factor and activation energy, respectively; and  $R$  is the universal gas constant (8.314 J mol K<sup>-1</sup>).

#### FWO method

The FWO model is a typical integral kinetic model that has been used extensively in literature [30, 32–35]. In Eq. (5),  $G(\alpha)$  is the integral of  $f(\alpha)^{-1}$ , and  $\beta$  is the heating rate. The activation energy can be calculated from the slope of the linear fitting line of  $\lg\beta$  and  $T^{-1}$ .

$$\lg\beta = \lg\left(\frac{AE_a}{RG(\alpha)}\right) - 2.315 - 0.4567\frac{E_a}{RT} \quad (5)$$

#### KAS method

The KAS model is an integral model based on the Coats–Redfern approximation, which is expressed in Eq. (6) [36, 37]. The value  $E_a$  can be obtained from the slope of the plot of  $\ln(\beta T^{-2})$  versus  $T^{-1}$ .

$$\ln\left(\frac{\beta}{T^2}\right) = \ln\frac{AR}{E_a G(\alpha)} - \frac{E_a}{R} \frac{1}{T} \quad (6)$$

### Vyazovkin method

Vyazovkin established an integral kinetic model based on the Arrhenius equation and type I kinetic equation. This model is expressed in Eq. (7) [30, 38].

$$-\ln t = \ln\frac{A}{G(\alpha)} - \frac{E_a}{R} \frac{1}{T} \quad (7)$$

### Starink method

The Starink method was established according to the consideration that the Kissinger model (Eq. (8)), Ozawa model (Eq. (9)), and Boswell model (Eq. (10)) can be generalized into a single formula [24]. After transformation and optimization, the Starink model was obtained. This model is expressed in Eq. (11) and is considered to be highly accurate for calculating  $E_a$  [26, 39]. The parameters  $C_K$ ,  $C_O$ ,  $C_B$ , and  $C_S$  are the constants of the equations of the Kissinger, Ozawa, Boswell, and Starink models, respectively.

$$\ln\left(\frac{\beta}{T^2}\right) = C_K - \frac{E_a}{R} \frac{1}{T} \quad (8)$$

$$\lg \beta = C_O - 1.0516 \frac{E_a}{RT} \quad (9)$$

$$\ln\left(\frac{\beta}{T}\right) = C_B - \frac{E_a}{R} \frac{1}{T} \quad (10)$$

$$\ln\left(\frac{\beta}{T^{1.8}}\right) = C_S - 1.0037 \frac{E_a}{R} \frac{1}{T} \quad (11)$$

## Results and analysis

### Thermokinetic analysis

Figure 1 displays the typical TGA results obtained for nitrocellulose. The curves under different oxygen content have similar variation tendency and the oxygen content in Fig. 1 is 5%. Only one major mass-loss period existed in the decomposition process. When the temperature exceeded 180 °C, the sample mass decreased by approximately 90% within a short time, as displayed in the derivative thermogravimetric (DTG) curves. The DTG peaks moved toward the high-temperature side as the heating rate increased, and the

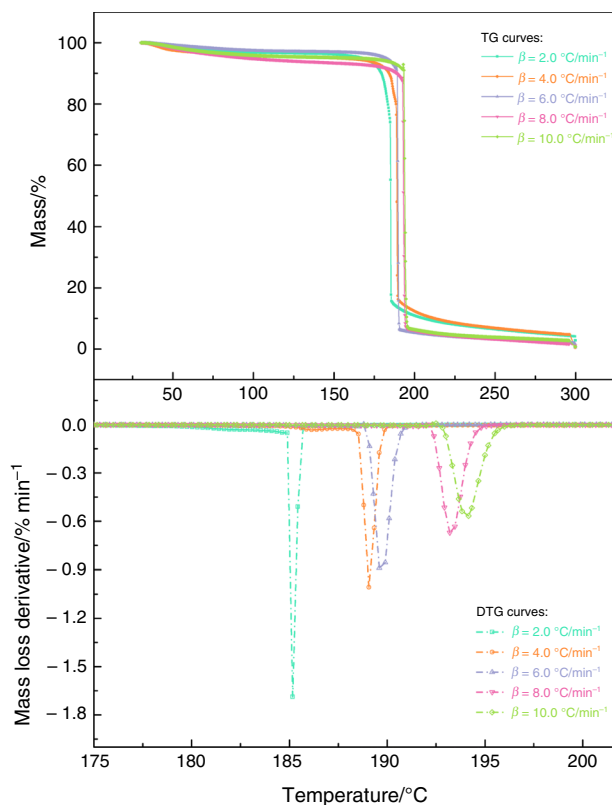


**Fig. 1** Thermogravimetric curves of nitrocellulose at 5% oxygen content

corresponding temperature increased to 184.90–194.52 °C. In addition, The TG curve also shows a slight increase at temperature around 190 °C when  $\beta$  was 10.0 °C min<sup>-1</sup>; it could be explained that large heat would be released rapidly at high heating rate, which could have led to a blast in the sample container. Consequently, the created reverse pressure was exerted on the inside scale of the TGA, leading to a transient increase in the sample mass.

By using the thermokinetic models mentioned in (“Thermokinetic models” section),  $E_a$  values can be obtained. Figure 2 shows the variation in  $E_a$  with conversion rate under different oxygen contents. The curves obtained using the KAS, FWO, Starink, and Vyazovkin methods exhibited synchronous variation, and the KAS and Starink curves almost coincided with each other. However, the Friedman curves exhibited certain differences and fluctuated over the conversion rate range of 0.3–0.8, especially when the oxygen content was 0%, 10%, and 15%, as illustrated in Fig. 2(a, c, and d), respectively. Table 1 lists the average  $E_a$  values and determination coefficients ( $R^2$ ) of the thermokinetic models under three oxygen content values. The average  $E_a$  obtained using the Friedman method was the smallest among all the methods, and the larger values obtained using the other four methods were close to each

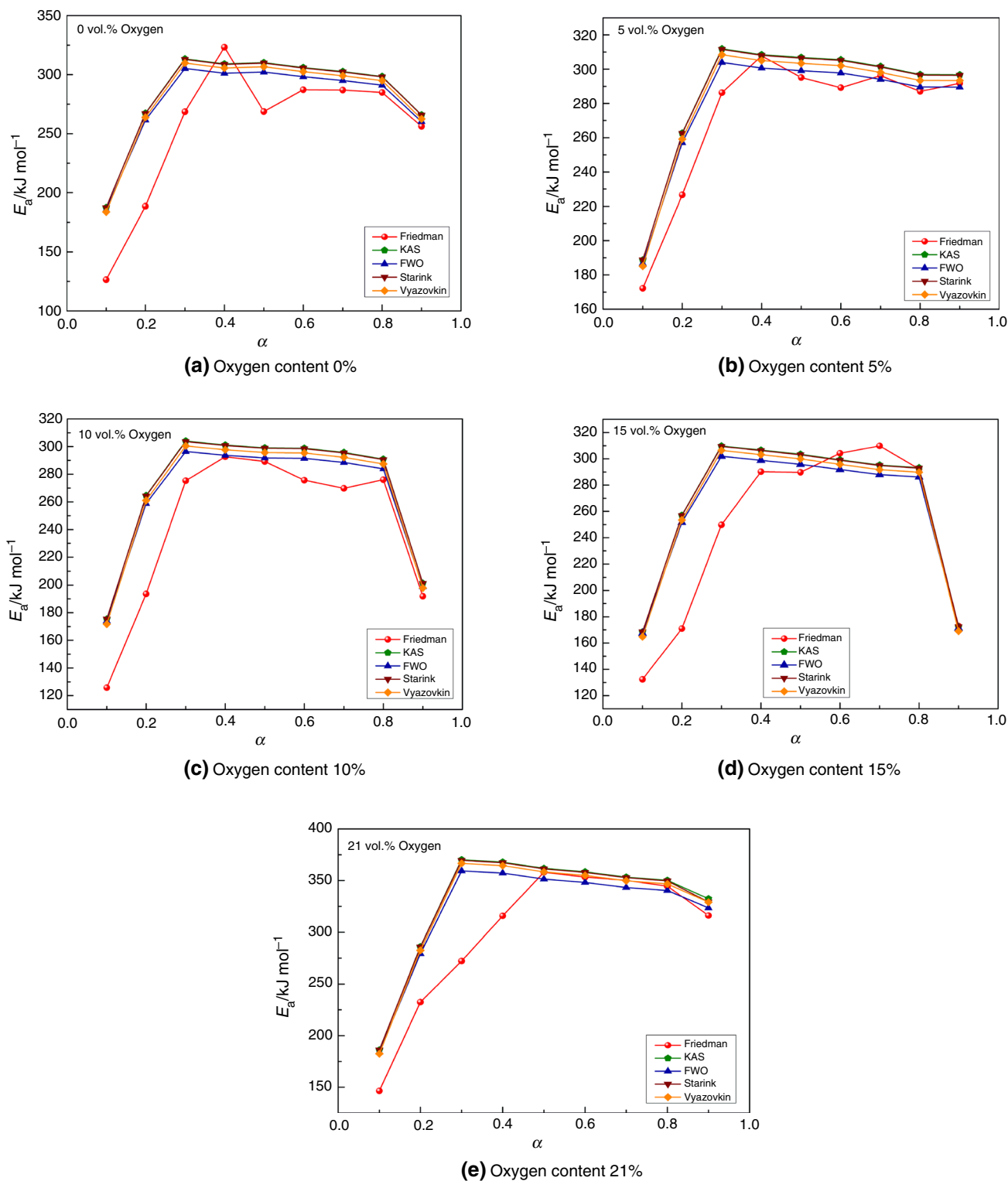


**Fig. 2** Variation in  $E_a$  with conversion rate under different oxygen contents: **a** 0%, **b** 5%, **c** 10%, **d** 15%, and **e** 21%

other. Moreover, the  $R^2$  value of the Friedman method was lower than those of the other four methods. Thus, compared with the KAS, FWO, Starink, and Vyazovkin models, the

Friedman model would not be very appropriate to calculate  $E_a$  of nitrocellulose using thermogravimetric data.

In addition, the  $E_a$  curves of the KAS, FWO, Starink, and Vyazovkin models indicate that the  $E_a$  had an

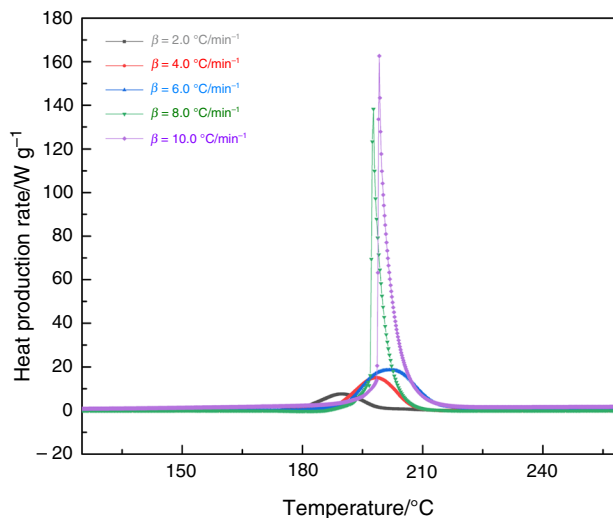
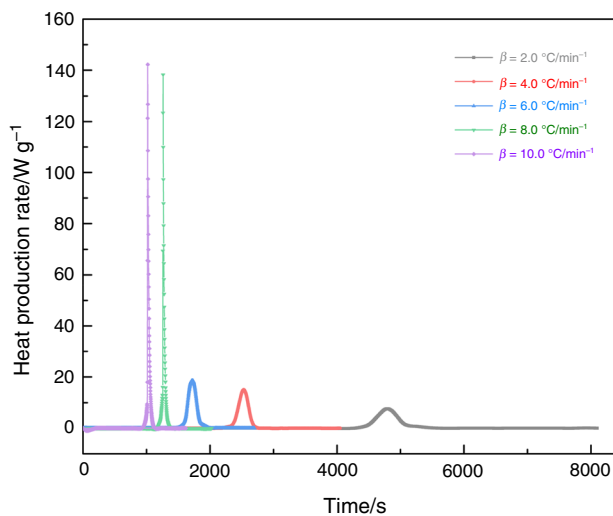
**Table 1** Average  $E_a$  and determination coefficient ( $R^2$ ) values of the five models under different oxygen contents

Methods	Oxygen 0%		Oxygen 10%		Oxygen 15%	
	$E_a/\text{kJ mol}^{-1}$	$R^2$	$E_a/\text{kJ mol}^{-1}$	$R^2$	$E_a/\text{kJ mol}^{-1}$	$R^2$
Friedman	254.53	0.9428	243.32	0.9611	245.81	0.9558
KAS	284.48	0.9582	270.09	0.9839	267.25	0.9578
FWO	277.83	0.9602	264.15	0.9847	261.45	0.9599
Starink	284.20	0.9584	269.86	0.9840	267.03	0.9580
Vyazovkin	280.98	0.9572	266.62	0.9835	263.78	0.9568

“increase–stabilize–decrease” tendency throughout the heating process. Similar results were reported in a previous study [40]. In the initial reaction period,  $E_a$  reached its minimum value under each oxygen content when the conversion rate was 0.1, which indicated that limited energy was required to activate the reaction. Therefore, necessary measures should be emphasized and implemented, especially at the beginning of nitrocellulose reaction. As the reaction proceeded,  $E_a$  increased dramatically and peaked when the conversion rate was 0.3. The average increase rate of  $E_a$  obtained using the four methods was up to 98% under an oxygen content of 21%. The  $E_a$  value then tended to stabilize as the conversion rate increased from 0.3 to 0.8. The average rate of variation in  $E_a$  was only 4.9% under different oxygen contents. When the conversion rate exceeded 0.8,  $E_a$  decreased with maximum and average change rates of 41% and 18%, respectively. The average  $E_a$  values under the oxygen contents of 0%, 5%, 10%, 15%, and 21% were calculated to be 281.87, 283.97, 276.17, 276.57, and 326.05  $\text{kJ mol}^{-1}$ , respectively, which indicated that the  $E_a$  values were relatively stable in oxygen-lean environments. The aforementioned  $E_a$  values are lower than that in the air. Similar results were obtained in a previous study for nitrocellulose solution (20–30 mass%), which was prepared by dissolving nitrocellulose in ethyl acetate [41].

### Thermal characteristic analysis

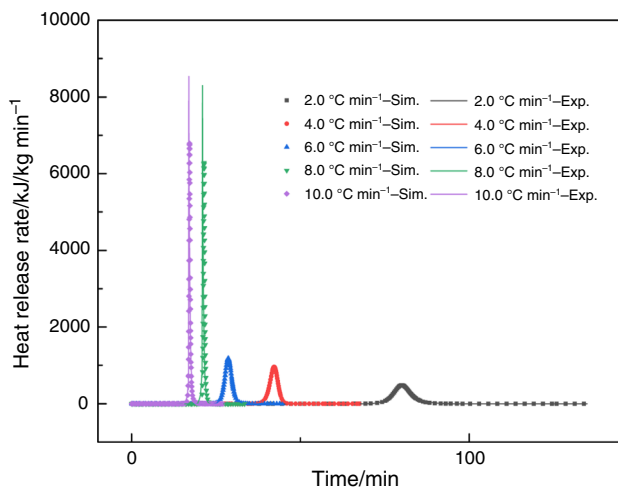
The heat production data of nitrocellulose under five heating rates ( $\beta$ ) were obtained through DSC, as illustrated in Figs. 3–4. The corresponding thermodynamic parameters are summarized in Table 2. Figure 3 and Table 2 indicate that the heat production curves moved toward the high-temperature side as  $\beta$  increased. The initial decomposition temperature  $T_0$  and maximum decomposition temperature  $T_p$  were 172.68–199.98 °C and 192.31–213.94 °C, respectively. These temperatures increased as  $\beta$  increased, and the trends of change in the maximum heat production and  $\beta$  were similar. According to Fig. 4, high reaction and heat production rates were achieved at large  $\beta$  values, especially those exceeding 6.0 °C  $\text{min}^{-1}$ , as indicated by the substantial increase in heat production under  $\beta$  values of 8.0–10.0 °C  $\text{min}^{-1}$ . Moreover, according to Table 2, the heat

**Fig. 3** Changes in the heat production rate of nitrocellulose with temperature**Fig. 4** Changes in the heat production rate of nitrocellulose with time

enthalpy under the heating rate of 6.0 °C  $\text{min}^{-1}$  was relatively high, with an average value of 3877.76  $\text{J g}^{-1}$ . The heating enthalpy was 3274.69  $\text{J g}^{-1}$  when  $\beta$  exceeded 6 °C  $\text{min}^{-1}$ . Thus, the thermal decomposition of nitrocellulose can

**Table 2** Thermodynamic parameters of nitrocellulose under different heating rates

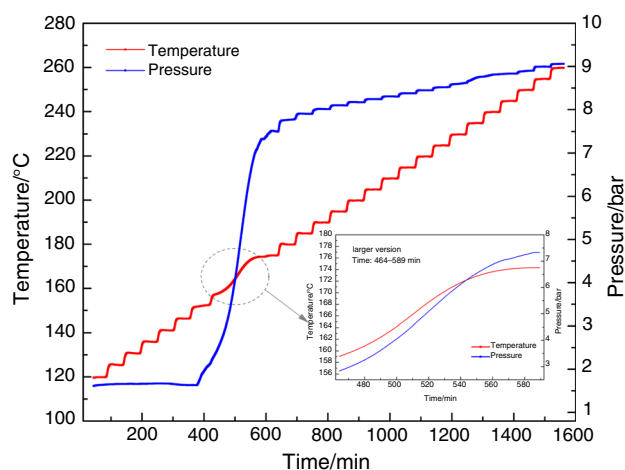
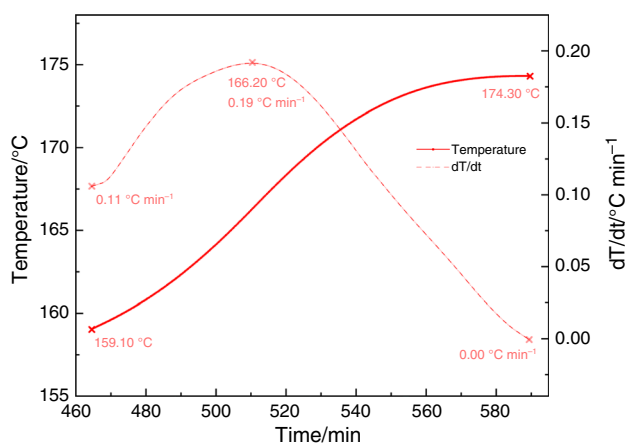
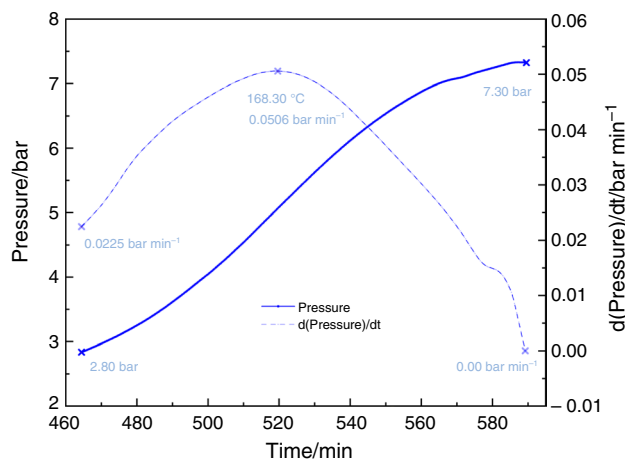
$\beta/^\circ\text{C min}^{-1}$	$T_0/^\circ\text{C}$	$T_p/^\circ\text{C}$	$\Delta H/J \text{ g}^{-1}$
2.0	172.68	192.31	3848.32
4.0	188.89	200.70	3975.44
6.0	192.14	204.98	3809.51
8.0	198.73	211.49	3315.94
10.0	199.98	213.94	3233.43

**Fig. 5** Comparison of the experimental and simulated data of the changes in heat release rate with time

release adequate heat when the environmental temperature increases at a slow rate. Therefore, suitable ventilation should be provided to prevent gradual heat accumulation during the storage and transportation of nitrocellulose.

For further exploring the reaction process and reaction mechanism of nitrocellulose, a one-step autocatalytic model was adopted to calculate the heat release rate during the thermal decomposition of nitrocellulose. The corresponding results are illustrated in Fig. 5, indicating high consistency between the simulation and experimental data. Therefore, the thermal decomposition of nitrocellulose in a nitrogen atmosphere is an “A → B” one-step autocatalytic reaction, which is consistent with the results reported in literature [16, 17].

Nitrocellulose was thermally decomposed under an adiabatic condition in ARC, as illustrated in Figs. 6–8. Figure 6 shows the complete temperature and pressure curves corresponding to this process; Fig. 7 displays the variations in the temperature and heating rate with time in the aforementioned decomposition process; and Fig. 8 depicts the variations in the pressure and the rate of pressure increases with time in the decomposition of nitrocellulose. The heating rate tended to first increase and then decrease. The maximum

**Fig. 6** Experimental curves obtained when performing ARC at a  $\beta$  value of  $10.0 \text{ }^\circ\text{C min}^{-1}$  for nitrocellulose**Fig. 7** Changes in the temperature and heating rate with time during the decomposition of nitrocellulose**Fig. 8** Changes in the pressure and the rate of pressure increase with time

heating rate was  $0.19\text{ }^{\circ}\text{C min}^{-1}$ , and the corresponding temperature was  $166.20\text{ }^{\circ}\text{C}$ . This heating rate corresponded to the maximum intensity of the decomposition reaction. During the decomposition process, the pressure in the confined container increased dramatically because of the release of heat and gaseous products. The trend of the rate of pressure increase was similar to that of the heating rate. The maximum pressure change rate was  $0.0506\text{ bar min}^{-1}$ , which occurred at a temperature of  $168.30\text{ }^{\circ}\text{C}$ .

During the ARC experiments, the heat released by nitrocellulose could be partly absorbed by the reactor. To compensate for this phenomenon, the factor of thermal inertia ( $\phi$ ) was introduced in the analysis. This factor represents the inertia of a substance against heat. High thermal inertia reduces the reaction rate and rate of temperature change. The  $\phi$  value of a reaction system is 1 under ideal conditions. For the experiments conducted in this study,  $\phi$  was calculated to be 47.538, which is considerably higher than the ideal value. Therefore, the adiabatic temperature rise  $\Delta T_{\text{ad}}$  obtained from the experiment was relatively small at  $15.20\text{ }^{\circ}\text{C}$ . The theoretical ideal  $T_{\text{ad}}$  value of a sample can be obtained using Eq. (12) [42, 43], and this value was up to  $722.58\text{ }^{\circ}\text{C}$  in this study.

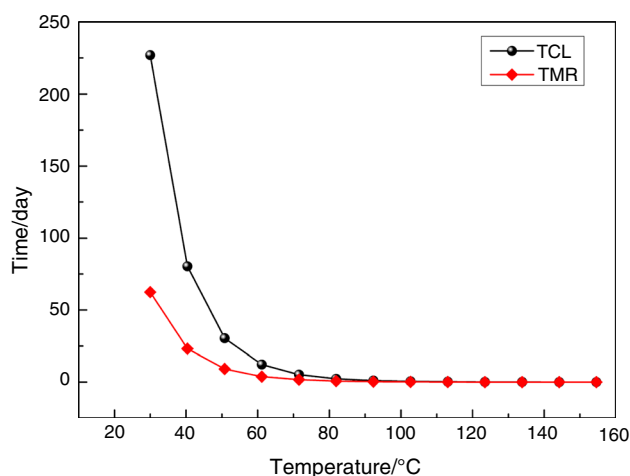
$$T_{\text{ad}}' = \phi \Delta T_{\text{ad}} \quad (12)$$

Table 3 presents the criteria for assessing the severity of thermal runaway [44, 45]. According to these criteria, the thermal runaway severity of nitrocellulose is catastrophic, which indicates that heavy damage would be caused by the violent reaction of nitrocellulose.

During the storage and transportation process, the thermal stability of a material can be considerably affected by the environmental temperature. Therefore, time to conversion limit (TCL) and time to reach the maximum reaction rate (TMR) were considered when evaluating the thermal stability of nitrocellulose [6, 46, 47]. These parameters were determined using the aforementioned one-step autocatalytic model (Fig. 9). A conversion limit of 10% was selected in this study. TCL and TMR decreased as the temperature increased, and a dramatic decrease was observed in these parameters when the temperature increased from 30 to  $60\text{ }^{\circ}\text{C}$ , which indicates that nitrocellulose has high-temperature sensitivity. The TCL and TMR were less than 24 h when the temperature exceeded  $93\text{ }^{\circ}\text{C}$  and  $79\text{ }^{\circ}\text{C}$ , respectively. When

**Table 3** Assessment criteria for the severity of thermal runaway of nitrocellulose

Level	$\Delta T_{\text{ad}}/^{\circ}\text{C}$	Criticality
1	< 50	Negligible
2	50–100	Medium
3	200–400	Critical
4	> 400	Catastrophic



**Fig. 9** The TCL and TMR of nitrocellulose versus temperature

the temperature exceeded  $100\text{ }^{\circ}\text{C}$ , the aforementioned parameters stabilized at extremely small values. Thus, a prompt reaction was achieved, consistent with the large mass-loss rates depicted in Fig. 1 and high heat production rates depicted in Figs. 3–4.

Self-accelerating decomposition temperature (SADT) is another vital safety parameter used in the thermal stability analysis of hazardous materials [28, 39, 48]. SADT is defined as the lowest environmental temperature at which a packaged chemical can decompose in a self-accelerating manner within 7.0 days. The SADT and reaction progress of nitrocellulose in a 50 kg package were determined (Fig. 10). The temperature at the center of the nitrocellulose package was  $6\text{ }^{\circ}\text{C}$  higher than the environmental temperature within 5.9 days of self-accelerated decomposition. The SADT was calculated to be  $49\text{ }^{\circ}\text{C}$ , which is similar to the values reported in literature [48]. According to the critical

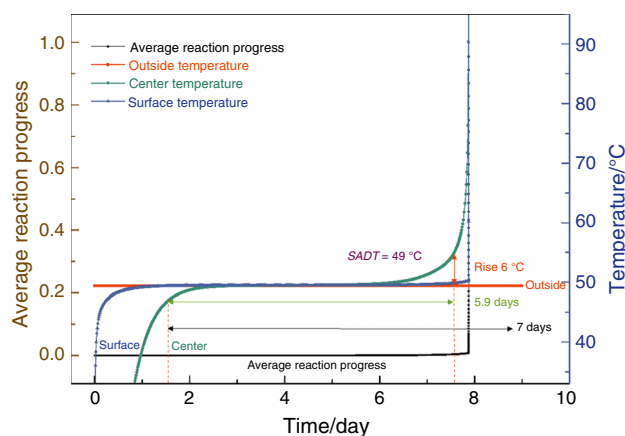


**Fig. 10** SADT and average reaction progress for a 50 kg package of nitrocellulose



**Table 4** Relationships between control temperature, alarm temperature, and SADT

$SADT/^\circ\text{C}$	Control temperature/ $^\circ\text{C}$	Alarm temperature/ $^\circ\text{C}$
$SADT \leq 20$	$< 20$	$SADT - 10$
$20 \leq SADT \leq 35$	$SADT - 15$	$SADT - 10$
$35 \leq SADT$	$SADT - 10$	$SADT - 5$

temperature relationship presented in Table 4 [28, 49], the control and alarm temperatures of nitrocellulose are 39 and 44 °C, respectively.

## Conclusions

In this study, the thermal stability of nitrocellulose was investigated through TGA, DSC, and ARC. The main conclusions of this study are as follows:

- (1) The activation energy ( $E_a$ ) of nitrocellulose under oxygen contents of 0%, 5%, 10%, 15%, and 21% was obtained using the Friedman, FWO, KAS, Starink, and Vyazovkin methods. The results revealed that  $E_a$  exhibited an “increase–stabilize–decrease” trend during thermal decomposition, and the  $E_a$  values in oxygen-lean environments were relatively stable and lower than that in air. Compared with Friedman method, the other four methods exhibited optimal applicability for  $E_a$  analysis based on TGA data.
- (2) The results of the DSC experiments indicated that the initial and maximum decomposition temperatures increased as  $\beta$  increased, and the heat enthalpy was higher under lower heating rates. The thermal decomposition of nitrocellulose in a nitrogen atmosphere was an “A  $\rightarrow$  B” one-step autocatalytic reaction.
- (3) The adiabatic temperature increase of nitrocellulose was obtained, and the thermal runaway severity of nitrocellulose was determined to be catastrophic. TCL and TMR decreased as the temperature increased, and their values were less than 24 h when the temperature exceeded 93 and 79 °C, respectively. The calculated SADT of a 50 kg package of nitrocellulose was 49 °C, and the control temperature was 39 °C, which is the upper-temperature limit for nitrocellulose storage.

**Acknowledgements** We thank the General Natural Science Research Project of Jiangsu University (Nos. 20KJB620002, 20KJD620001), 2020 Industrial Technology Foundation Public Service Platform Project (2020-0107-3-1), and National Nature Science Foundation (No. 21927815) for financially supporting this study. We also thank National Yunlin University of Science and Technology for the technical support.

## References

1. Pourmortazavi SM, Hosseini SG, Rahimi-Nasrabadi M, Hajimirsadeghi SS, Momenian H. Effect of nitrate content on thermal decomposition of nitrocellulose. *J Hazard Mater.* 2009;162(2–3):1141–4.
2. Gao X, Jiang L, Xu Q. Experimental and theoretical study on thermal kinetics and reactive mechanism of nitrocellulose pyrolysis by traditional multi kinetics and modeling reconstruction. *J Hazard Mater.* 2020;386:121645.
3. Brill TB, Gongwer PE. Thermal decomposition of energetic materials 69. Analysis of the kinetics of nitrocellulose at 50°C–500°C. *Propellants Explos Pyrotech.* 1997;22(1):38–44.
4. Hassan MA. Effect of malonyl malonanilide dimers on the thermal stability of nitrocellulose. *J Hazard Mater.* 2001;88(1):33–49.
5. Sovizi MR, Hajimirsadeghi SS, Naderizadeh B. Effect of particle size on thermal decomposition of nitrocellulose. *J Hazard Mater.* 2009;168(2–3):1134–9.
6. Wei RC, Huang SS, Wang Z, He Y, Yuen R, Wang J. Estimation on the safe storage temperature of nitrocellulose with different humectants. *Propellants Explos Pyrotech.* 2018;43(11):1122–8.
7. Chen QL, Wood M, Zhao JS. Case study of the Tianjin accident: Application of barrier and systems analysis to understand challenges to industry loss prevention in emerging economies. *Process Saf Environ Prot.* 2019;131:178–88.
8. Wang J, Fu G, Yan M. Comparative analysis of two catastrophic hazardous chemical accidents in China. *Process Saf Prog.* 2020;39(1):e12137.
9. Yang Y, Ding L, Xu L, Tsai YT. Effect of metal chloride on thermal decomposition of nitrocellulose. *Case Stud Therm Eng.* 2021;28:101667.
10. Guo S, Wang QS, Sun JH, Liao X, Wang ZS. Study on the influence of moisture content on thermal stability of propellant. *J Hazard Mater.* 2009;168(1):536–41.
11. Katoh K, Ito S, Ogata Y, Kasamatsu J, Miya H, Yamamoto M, et al. Effect of industrial water components on thermal stability of nitrocellulose. *J Therm Anal Calorim.* 2010;99(1):159–64.
12. Katoh K, Higashi E, Nakano K, Ito S, Wada Y, Kasamatsu J, et al. Thermal behavior of nitrocellulose with inorganic salts and their mechanistic action. *Propellants Explos Pyrotech.* 2010;35(5):461–7.
13. Lin CP, Chang YM, Gupta JP, Shu CM. Comparisons of TGA and DSC approaches to evaluate nitrocellulose thermal degradation energy and stabilizer efficiencies. *Process Saf Environ Prot.* 2010;88(6):413–9.
14. Luo LQ, Huang Q, Jin B, Chai ZH, Guo ZL, Peng RF. Study on the stability effect and mechanism of aniline-fullerene stabilizers on nitrocellulose based on the isothermal thermal decomposition. *Polym Degrad Stab.* 2020;178:109221.
15. Zhang X, Weeks BL. Preparation of sub-micron nitrocellulose particles for improved combustion behavior. *J Hazard Mater.* 2014;268:224–8.
16. Guo PJ, Hu RZ, Ning BK, Yang ZQ, Song JR, Shi QZ, et al. Kinetics of the first order autocatalytic decomposition reaction of nitrocellulose (13.86% N). *Chin J Chem.* 2004;22(1):19–23.
17. Ning BK, Hu RZ, Zhang H, Xia ZM, Guo PJ, Liu R, et al. Estimation of the critical rate of temperature rise for thermal explosion of autocatalytic decomposing reaction of nitrocellulose using non-isothermal DSC. *Thermochim Acta.* 2004;416(1–2):47–50.
18. Cherif MF, Trache D, Benaliouche F, Tarchoun AF, Chelouche S, Mezroua A. Organosolv lignins as new stabilizers for cellulose nitrate: thermal behavior and stability assessment. *Int J Biol Macromol.* 2020;164:794–807.
19. Wang H, Zhang H, Hu R, Yao E, Guo P. Estimation of the critical rate of temperature rise for thermal explosion of

- nitrocellulose using non-isothermal DSC. *J Therm Anal Calorim.* 2014;115(2):1099–110.
20. He Y, He YP, Liu JH, Li P, Chen MY, Wei RC, et al. Experimental study on the thermal decomposition and combustion characteristics of nitrocellulose with different alcohol humectants. *J Hazard Mater.* 2017;340:202–12.
  21. Luo QB, Ren T, Shen H, Zhang J, Liang D. The thermal properties of nitrocellulose: from thermal decomposition to thermal explosion. *Combust Sci Technol.* 2018;190(4):579–90.
  22. Mi WZ. Ignition characteristics and case analysis of typical nitrocellulose. Anhui: University of Science and Technology of China; 2018.
  23. Wei RC, Huang SS, Wang Z, Wang XH, Ding C, Yuen R, et al. Thermal behavior of nitrocellulose with different aging periods. *J Therm Anal Calorim.* 2019;136(2):651–60.
  24. Hu RZ, Shi QZ. Thermal analysis kinetics. Beijing: Science Press; 2001.
  25. Zhong XX, Li L, Chen Y, Dou GL, Xin HH. Changes in thermal kinetics characteristics during low-temperature oxidation of low-rank coals under lean-oxygen conditions. *Energ Fuel.* 2017;31(1):239–48.
  26. Vyazovkin S, Burnham AK, Criado JM, Pérez-Maqueda LA, Popescu C, Sbirrazzuoli N. ICTAC kinetics committee recommendations for performing kinetic computations on thermal analysis data. *Thermochim Acta.* 2011;520(1–2):1–19.
  27. Mandal S, Mohalik NK, Ray SK, Khan AM, Mishra D, Pandey JK. A comparative kinetic study between TGA & DSC techniques using model-free and model-based analyses to assess spontaneous combustion propensity of Indian coals. *Process Saf Environ Prot.* 2022;159:1113–26.
  28. Zhou HL, Jiang JC, Huang AC, Tang Y, Zhang Y, Huang CF, et al. Calorimetric evaluation of thermal stability and runaway hazard based on thermokinetic parameters of O, O-dimethyl phosphoramidithioate. *J Loss Prev Process Ind.* 2022;75:104697.
  29. Friedman HL. Kinetics of thermal degradation of char-forming plastics from plastics from thermogravimetry. Application to a phenolic plastic. *J Polym Sci Part C: Polym Symp.* 1964;6(1):183–95.
  30. Vyazovkin S, Sbirrazzuoli N. Isoconversional kinetic analysis of thermally stimulated processes in polymers. *Macromol Rapid Commun.* 2006;27(18):1515–32.
  31. Huang AC, Chen WC, Huang CF, Zhao JY, Deng J, Shu CM. Thermal stability simulations of 1, 1-bis (tert-butylperoxy)-3, 3, 5 trimethylcyclohexane mixed with metal ions. *J Therm Anal Calorim.* 2017;130(2):949–57.
  32. Li X, Yao HJ, Lu X, Chen C, Cao YZ, Xin Z. Effect of pyrogallol on the ring-opening polymerization and curing kinetics of a fully bio-based benzoxazine. *Thermochim Acta.* 2020;694:178787.
  33. Bai ZJ, Wang CP, Deng J, Kang FR, Shu CM. Experimental investigation on using ionic liquid to control spontaneous combustion of lignite. *Process Saf Environ Prot.* 2020;142:138–49.
  34. Cao CR, Liu SH, Huang AC, Lee MH, Ho SP, Yu WL, et al. Application of thermal ignition theory of di (2, 4-dichlorobenzoyl) peroxide by kinetic-based curve fitting. *J Therm Anal Calorim.* 2018;133(1):753–61.
  35. Liu SH, Shu CM. Advanced technology of thermal decomposition for AMBN and ABVN by DSC and VSP2. *J Therm Anal Calorim.* 2015;121:533–40.
  36. Coats AW, Redfern JP. Kinetic parameters from thermogravimetric data. *Nature.* 1964;201(4914):68–9.
  37. Tankov I, Yankova R, Mitkova M, Stratiev D. Non-isothermal decomposition kinetics of pyridinium nitrate under nitrogen atmosphere. *Thermochim Acta.* 2018;665:85–91.
  38. Vyazovkin S, Wight CA. Model-free and model-fitting approaches to kinetic analysis of isothermal and nonisothermal data. *Thermochim Acta.* 1999;340:53–68.
  39. Huang AC, Li ZP, Liu YC, Tang Y, Huang CF, Shu CM, et al. Essential hazard and process safety assessment of para-toluene sulfonic acid through calorimetry and advanced thermokinetics. *J Loss Prev Process Ind.* 2021;72:104558.
  40. Zhao NN, Ma H, An T, Zhao F, Hu R. Effects of superthermite Al/Fe<sub>2</sub>O<sub>3</sub> on the thermal decomposition characteristics of nitrocellulose. *Chin J Explos.* 2016;39:84–92.
  41. Li ZP, Jiang JC, Huang AC, Tang Y, Miao CF, Zhai J, et al. Thermal hazard evaluation on spontaneous combustion characteristics of nitrocellulose solution under different atmospheric conditions. *Sci Rep.* 2021;11(1):1–13.
  42. Qian XM, Liu L, Zhang J. Accelerating rate calorimeter and its application in the thermal hazard evaluation of chemical production. *J Saf Sci Technol.* 2005;1:13–8.
  43. Townsend DI, Tou JC. Thermal hazard evaluation by an accelerating rate calorimeter. *Thermochim Acta.* 1980;37(1):1–30.
  44. Stoessel F. Thermal safety of chemical processes: risk assessment and process design. New York: Wiley; 2008.
  45. Liu SH, Lu YM, Su C. Thermal hazard investigation and hazardous scenarios identification using thermal analysis coupled with numerical simulation for 2-(1-cyano-1-methylethyl) azocarboxamide. *J Hazard Mater.* 2020;384:121427.
  46. Huang AC, Huang CF, Xing ZX, Jiang JC, Shu CM. Thermal hazard assessment of the thermal stability of acne cosmeceutical therapy using advanced calorimetry technology. *Process Saf Environ Prot.* 2019;131:197–204.
  47. Liu YC, Jiang JC, Huang AC, Tang Y, Yang YP, Zhou HL, et al. Hazard assessment of the thermal stability of nitrification by-products by using an advanced kinetic model. *Process Saf Environ Prot.* 2022;160:91–101.
  48. Chai H, Duan QL, Cao HQ, Li M, Qi KX, Sun JH, et al. Experimental study on the effect of storage conditions on thermal stability of nitrocellulose. *Appl Therm Eng.* 2020;180:115871.
  49. Guo L, Xie CX, Huang F, Zhang JM, Li ZC. On the thermal safety and stability of dicumyl peroxide. *J Saf Environ.* 2013;13(1):211–4.

**Publisher's Note** Springer Nature remains neutral with regard to jurisdictional claims in published maps and institutional affiliations.

Springer Nature or its licensor (e.g. a society or other partner) holds exclusive rights to this article under a publishing agreement with the author(s) or other rightsholder(s); author self-archiving of the accepted manuscript version of this article is solely governed by the terms of such publishing agreement and applicable law.